

MODELING / MEASUREMENT COMPARISON OF SIGNAL COLLECTION IN DIAMOND SENSORS IN EXTREME CONDITIONS

V. Kubyskiy*, S. Liu, P. Bambade, LAL, Université Paris-Sud, CNRS/IN2P3, Orsay, France

Abstract

Such unique properties like radiation hardness, low dark current, good signal to noise ratio make single crystal Diamond Sensors (DS) excellent devices for measurements of beams in a wide range of conditions. Here we present a study of charge collection dynamics in a DS subjected to intensities from 1 to 10^9 Minimum Ionizing Particles (MIP). We developed a model based on the numerical solution of the 1D drift-diffusion equations, using the Scharfetter-Gummel discretization scheme. Inhomogeneity of the space-charge distribution together with the externally applied electric field are taken into account by analytically solving the Poisson equation at each discrete time step. We identified two regimes of charge collection. The first corresponds to $1 - 10^6$ MIPs, in this case the externally applied electric field is negligibly perturbed by space-charge effects during the separation of the electron/hole clouds. The second corresponds to intensities larger than 10^7 MIPs, where the space-charge effects significantly slow down the charge collection due to large concentrations of electron/hole pairs in the DS volume. The results of our modeling are in qualitative agreement with the experimental data acquired at the PHIL photo-injector electron beam facility at LAL. Our model allows optimising DS parameters to achieve desired charge collection times for different beam intensities.

INTRODUCTION

When charged particles pass through the material it ionises the material along the track which results in the creation of electron hole pairs. In the case of diamond, 1 MIP creates on average 36 electron-hole pairs per micrometer. Applying external electric field to the diamond force the electrons and holes to move in opposite directions, this process is usually called charge collection. According to Shockley-Ramo theorem [1] the motion of these charges creates an electric current on the electrodes which can be amplified if it is necessary and measured with an oscilloscope.

However when the diamond sensor is subjected to the beam where the number of electrons (MIPs) can be as large as 10^8 electrons or more, the charge collection becomes nonlinear and it can be strongly slowed down (see [2]) for the following reasons: First, is the space charge effect that becomes important when the clouds of electron and holes are separated in the external electric field, which creates an opposite electric field to the applied one inside the sensor. Second, is the voltage drop due to the strong current which passes through the resistive load in the readout channel.

In this paper we construct a Diamond Sensor model which includes these effects in a consecutive manner. Modeling of

* kubyskiy@lal.in2p3.fr

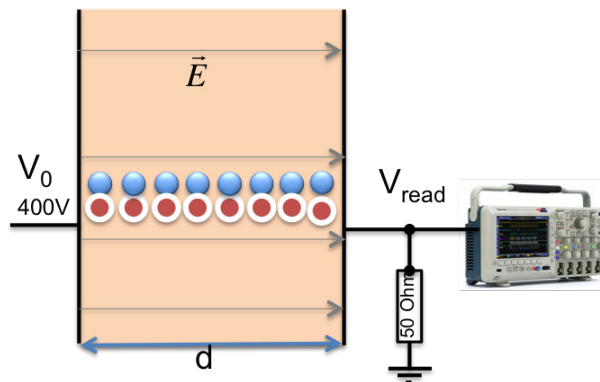


Figure 1: Schematic representation of diamond detector with electronics for data acquisition. Electrons (blue circles) and holes (red circles) pairs are created along the track of the incident MIP.

charge collection in diamond sensors subjected to extreme conditions is of great importance for the device parameter specification during the design and for calibration during operation.

MODELLING OF CHARGE COLLECTION

Let us consider the 1D case where the detector has a finite thickness and is infinite in the lateral directions. In this case the Poisson equation can be solved analytically, giving the electric field inside the material:

$$E(x,t) = -\frac{V}{d} - \frac{q}{\epsilon_0 d} \int_0^d \int_0^x (p-n) dx' dx + \frac{q}{\epsilon_0} \int_0^x (p-n) dx', \quad (1)$$

where

$$V = V_0 - V_{read} \quad (2)$$

is the difference of potentials applied to the diamond due to polarising potential V_0 and voltage drop on the reading electrode V_{read} ; n and p are electrons and holes densities, d is the thickness of the diamond; q is the elementary charge and ϵ_0 is dielectric constant.

In order to obtain temporal evolution of charge densities in the volume of the diamond we are solving the drift-diffusion equations [3]:

$$\frac{\partial J_n}{\partial x} - q \frac{\partial n}{\partial t} = \frac{n}{\tau_n} \quad \text{with } J_n = qn\mu_n E + qD_n \frac{\partial n}{\partial x}, \quad (3)$$

$$\frac{\partial J_p}{\partial x} + q \frac{\partial p}{\partial t} = -\frac{p}{\tau_p} \quad \text{with } J_p = qp\mu_p E + qD_p \frac{\partial p}{\partial x}, \quad (4)$$

where, correspondingly for electrons and holes, J_n and J_p are electric current densities; μ_n and μ_p are the mobilities; D_n , D_p diffusion constants and τ_n , τ_p lifetimes.

Content from this work may be used under the terms of the CC BY 3.0 licence (© 2015). Any distribution of this work must maintain attribution to the author(s), title of the work, publisher, and DOI.

We are working in the approximation in which the level of material ionisation is proportional to the number of particles in the beam. Accordingly, we define initial conditions as a homogeneous electron/holes distribution multiplied by number of incident particles. On the boundaries of the material (electrodes sides) we defined Dirichlet boundary conditions, which are representing absence of the charges caused by ionisation. The system of Eqns. 3-4 together with calculation of the instantaneous electric field inside the material for a given distribution of electrons and holes in the material (Eq. 1) can now be solved numerically. To avoid direct solving of the second order partial differential equations we used the Scharfetter-Gummel [4] discretization scheme. We calculate current in the intermediate nodes of the spatially discretized electron/holes densities:

$$J_n(x_{i+1/2}, t) = v \frac{n(x_i, t) - \exp(-v\Delta x/D)n(x_{i+1}, t)}{1 - \exp(-v\Delta x/D)}, \quad (5)$$

$$v = \frac{\mu E}{1 + \frac{\mu E}{v^{sat}}}, \quad (6)$$

where v is the local velocity of charge carriers and v^{sat} is the saturation velocity. The spatial derivative of the electric current density can be written as $\frac{\partial J_n}{\partial x} = \frac{J_n(x_{i+1/2}, t) - J_n(x_{i-1/2}, t)}{\Delta x}$.

The parameters in our model are: number of incident particles N_{mip} , biased voltage V_0 and the diamond thickness d . Solution of Eqns. (1-4) with standard Runge-Kutta method gives us temporal evolution and spatial distribution of: $n(x, t)$, $p(x, t)$, $J_n(x, t)$, $J_p(x, t)$ and $E(x, t)$.

DIAMOND SENSOR IN EXTREME CONDITIONS

Diamond sensors have a very large dynamic range, in principle from 1 MIP to 10^{10} MIPs (upper range is not well defined yet), large part of this range (1- 10^6) demonstrates linear response, waveforms scaling with the number of incident particles and similar charge collection times (blue curve in Fig. 2). However for more intense beams the charge collection can be significantly slowed down (red curve in Fig. 2).

The parameters that we used in our modelling are listed in the Table 1.

Our first simulations have shown that when $N_{mip} \leq 10^5$ $V_{read} \ll V_0$. When $N_{mip} = 10^6$, $V_{read} \approx 25$ V, which still does not strongly affect the charge collection dynamics. However, when $N_{mip} > 10^6$ the signal V_{read} reaches values which can exceed V_0 , which are unphysical and contradictory with our measured signals (Fig. 2), where V_{read} at maximum can reach the values close to V_0 . The qualitative picture of the process is the following: immediately after material ionisation at the moment $t = 0$ electrons and holes start to move in opposite directions in the externally applied electric field (reaching rapidly they saturation velocities), creating electric current I on the reading electrode.

Table 1: Model Parameters

Global parameters	Number of MIPs N_{mip}	varies
	Biased voltage V_0	400 V
	Diamond thickness d	500 μm
Material parameters [5]	Mobility μ_n	2000 cm^2/Vs
	Mobility μ_p	2300 cm^2/Vs
	Saturation velocity v_n^{sat}	$1e6 - 1.9e7$ cm/s
	Saturation velocity v_p^{sat}	$1e6 - 1.4e7$ cm/s
	Lifetime τ_n	100 - 300 ns
	Lifetime τ_p	100 - 300 ns

Roughly saying, this induced electric current is a "projection" of charge carriers motion on the electrode. Applying Schokley-Ramo theorem [1], and integrating all the contributions from moving charges in the volume one can obtain induced electric current I on the reading electrode.

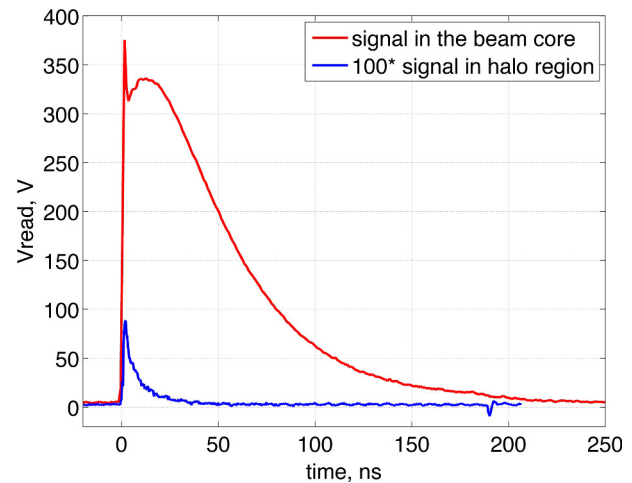


Figure 2: Charge collection by diamond sensor, bias voltage is 400V. Red: typical waveform in the beam core, $N_{mips} \approx 10^9$. Blue: typical waveform in the halo region with scaling factor of 100, N_{mips} is of the order of few thousands.

The instantaneous current creates a voltage drop on the grounded 50 Ohm resistor. A strong output current I due to the applied potential V_0 leads to a strong voltage drop, which reduces the difference of potentials V (see Eq.2) and slows down the charge collection and current pulse. And *vice versa*: weak current I leads to small V_{read} , which gives $V \approx V_0$ leading to fast charge collection and finally to large I . Our considerations above demonstrate that the V_{read} and the dynamical process of charge collection must be self-consistent, which can be expressed as:

$$V_{read} = f(I(V_{read})). \quad (7)$$

Solving Eq. (7) at each modelling time step we obtain the value of V_{read} for which charge collection and voltage drop are self-consistent.

RESULTS

The simulated charge collection curves for $N_{mips} = 10^7$: $2 \cdot 10^9$ are presented in Fig. 3. Increasing of N_{mips} increases the magnitude of V_{read} (discussed in previous section) as well as the duration of the charge collection.

Charge collection efficiency (CCE) for $N_{mips} = 10^7$ is 35%, whereas for $N_{mips} = 2 \cdot 10^7$ is decreasing to 15%. In our simulations the only reason for CCE to be less than 100% is due to the finite lifetimes of electrons and holes, appearing in the RHS of continuity eqns. 3-4. Here we are considering lifetimes which take into account all possible sources of charge losses such as recombination, optical phonon scattering, scattering on the defects etc.

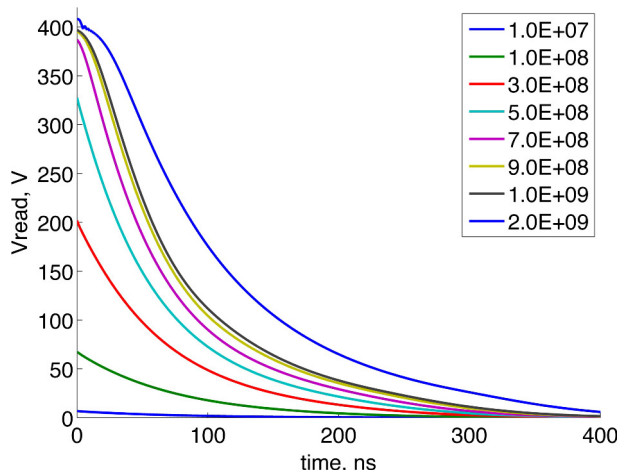


Figure 3: Modelling of DS signals for different number of incident electrons N_{mip} .

Simulation results show reasonably good agreement with our measurements (Fig. 4). One can see that the simulation does not reproduce completely the behaviour of the measured waveform at the beginning of the pulse. This is a direct consequence of the way how we imposed self-consistency in Eq. 7, since we search for the settled value of V_{read} at each modelling time step without taking into account the dynamical nature of this process.

The space-charge effect is important factor in the charge collection slowdown. During the first two hundred nanoseconds slowdown is due to V_{read} (see Fig.4). However, even when V_{read} reached values as low as 25 V, the charge collection does not follow the same scenario as it would do for lower number of MIPs with initial peak value at 25 V. Such behaviour is due to the spatial distribution of electrons and holes. Since the mobilities of electrons and holes in the diamond are approximately the same, the large part of these charges forms "self-screening" zone around the center of the detector. It appears that such charge distribution is preferable by the system for keeping the charge collection. Later, when the applied voltage is sufficient to separate space-charge zone these charges are collected.

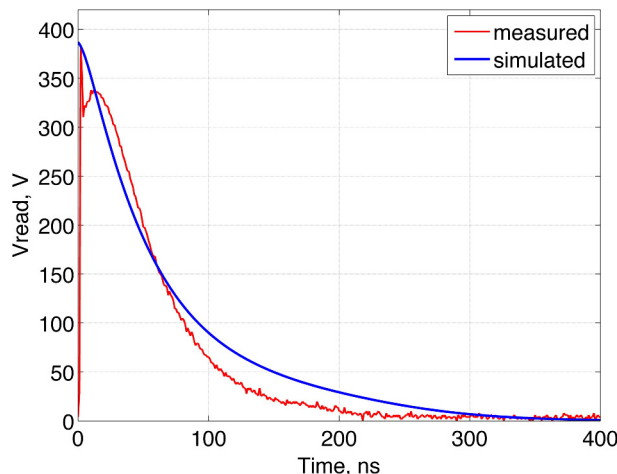


Figure 4: Comparison of simulation with measurements. Adjustment of the saturation velocities was made to achieve this results (for parameter see. Table 1).

CONCLUSIONS

We developed a 1D diamond sensor model which takes into account space-charge effects and instantaneous decrease of the voltage applied to the diamond during charge collection. These are the two principal sources of increase of the charge collection time. Up to 10^6 MIPs the charge collection is linear, whereas for larger intensities charge collection becomes nonlinear. With modelling we have access to the information about the temporal evolution and spatial distribution of the electrons and holes, which is crucial for the understanding and interpretation of the measured signals. Our model allows to determine the proper calibration of the diamond sensor signal with respect to number of incident particles, and can be used for the optimisation of the detector parameters for given application.

Our future plans are to improve DS model to operate with material parameters closer to the real ones and to understand the validity of Eq. 7.

ACKNOWLEDGMENT

Authors would like to thank for useful discussions to Erich Griesmayer and Didier Jehanno.

REFERENCES

- [1] W. Shockley, *Currents to Conductors Induced by a Moving Point Charge*, Journal of Applied Physics 9 (10) (1938).
S. Ramo, *Currents induced in electron motion*, PROC. IRE 27, 584 (1939).
- [2] S. Liu et al., *Investigation of beam halo using in vacuum diamond sensor at ATF2*, Proceedings IPAC'15 , MOPHA008, Richmond, USA (2015).
- [3] P.A. Markowich, C.A. Ringhofer, C. Schmeiser, *Semiconductor equations*, (Springer-Verlag New York, Inc. 1990).
- [4] D. L. Scharfetter and H. K. Gummel, *Large-signal analysis of a silicon read diode oscillator*, IEEE Transactions on Electron Devices 16, no. 1, 64-77 (1969).
- [5] M. Pomorski et al. *Charge transport properties of single crystal CVD-diamond particle detectors*. Diamond and related materials 16.4, 1066-1069 (2007).